Supplemental Information.

Plasmid Constructs. Plasmids pSPCFTR, pSPTM1-6, and pSPTM1-2, and are described elsewhere (Xiong. et al., 1997. J. Clin. Invest. 100: 1079-1088). PTrc-p47, and pQE-p97 were generously provided by Dr. Hemmo Meyer. Coding sequences for p97 and p47 were subcloned into Nco1 and BamH1 sites in frame to the His-6 tag of pET15b (EMD Biosciences, San Diego, CA) for heterologous expression.

Plasmids encoding His6-tagged CFTR NBD1 and NBD1-R domains were constructed as follows. CFTR residues V358-S589 were amplified by PCR using sense (TTTCCCTCCATGGTACAAACATGGTATGAC) and antisense (AGTTTCTGCAGCTAGCTTTCAAATATTTCTT) primers and ligated into NcoI/BamHI sites of a modified pSP64 plasmid described elsewhere (Skach, et al., Cancer Research, 54:3202-3209, 1994). Primers introduced an in-frame ATG translational start codon (NcoI site) immediately before CFTR codon V358 and a TAG stop codon at CFTR residue C590. Plasmid pSPNBD1 thus contains the coding sequence of NBD1 downstream of the SP6 promoter of pSP64. This construct pSPNBD1was then used as the template for a second PCR amplification using the same sense primer and an antisense primer (GAAGGATCCTCAGTGATGATGATGGTGGTGGCTTTCAAATATTTCTTT) encoding six in-frame His codons immediately upstream of a TGA stop codon. The PCR product was digested with BamHI and the resulting 414 BP BamHI fragment was ligated into BamHI-digested pSPNBD1 plasmid to generate pSPNBD1His_6.

Plasmid pSPNBD1-R was generated by ligating a BamHI/PvuII fragment (PvuII site is in pSP64 vector) from pSPCFTR836X, which encodes a TAG stop codon at residue D836

(Xiong, et al., J. Clin. Invest. 100:1079-1088, 1997), into BamHI/PvuII digested pSPNBD1. The resulting plasmid, encoding CFTR residues V358 to D835, was then used as a PCR template with sense (TTTCCCTCCATGGTACAAACATGGTATGAC) and antisense (AGACAGCTGTTAATGATGGTGGTGATGATGATCAAAAAGGCACTCCTT) primers. The antisense primer encodes $(His)_6$Val, immediately upstream of the stop codon followed by an engineered PvuII site. This fragment was digested with BamHI and PvuII and inserted into BamHI/PvuII digested pSPNBD-R, yielding NBD-R with a C-terminal His_6-tag.

Plasmid $pETUb^{G76V}$ was made by amplifying the human ubiquitin cDNA coding sequence (gift of Dr. M. Hochstrasser) with sense primer (AAGACTTCATGATGCAGATCTTCGTCAAC) and antisense primer (AACCAGCCATGGCCACACCTCTTAGTCTTAAGAC), digesting with NcoI and BspHI, and ligating into an NcoI digested pET15b vector. The antisense primer also introduced a G to V mutation at Ubiquitin codon 76. Plasmid pETUb-ubcH5a was then made by amplifying ubcH5a (gift of Dr. Peter Howley) with sense primer (TGACCCATGGCGCTGAAGAGGATT) and antisense primer (TCCGGCGGATCCTTAGTGATGATGATGATGATGCATTGCATATTTCTGAGT), digesting with NcoI and BamHI and ligating between the NcoI and BamHI sites of $pET15ub^{G76V}$. The resulting in pET15Ub-ubcH5a ecodes a non-cleavable ubiqutin fusion protein with a C-terminal His_6 tag.

TM1-2 (E92A/K95A) was amplified from plasmid pSPCFTR E92A/K95A (Lu et al., J. Biol. Chem. 273:658-576,1998) with sense primer (AGGATCTGGCTAGCGATCACC)

and antisense primer (GTTCAGGTTTCACGTCACCTTGTTGGAAAGGAGACT), and the resulting DNA fragment was used directly in transcription reactions.

Recombinant protein production. Recombinant protein expression was induced in transformed BL21(DE3) cultures using 0.4mM isopropyl β-D-1-thiogalactopyranoside (IPTG; Fisher Scientific, Pittsburgh, PA) as previously described (Carlson et al., 2005). Cell lysates were loaded onto a 5 ml Ni-NTA column (Qiagen, Inc., Valencia, CA), washed with 50 ml 300mM NaCl, 1mM βME, 5% glycerol, 0.4mM PMSF, 25mM imidazole, and 50mM Tris-HCl, pH 7.5, and eluted with a 25mM-500mM linear gradient of imidazole. Fractions were pooled, dialyzed against 100mM NaCl, 1mM βME, and 25mM Tris-HCl, pH 7.5 (Buffer A), then concentrated and stored at –80^{O}C. Aliquots were thawed once and discarded.

Immunoblots. Following depletion, RRL or CRMs were separated by SDS-PAGE, transferred to nitrocellulose or PVDF, and blotted with mouse α–p97 (1:500; BD Transduction Laboratories, San Jose, CA), mouse α-Rpt5 (1:2,500 BioRad), α-c9 antisera (1:2,500; [Oberdorf, 2006 #1257]) or mouse α-ufd1 (1:1,000; BD Transduction Laboratories) followed by α-mouse- or α-rabbit HRP secondary Ab (1:20,000. Biorad, Hercules, CA). The blots were imaged on Kodak film using Pierce west pico supersignal substrate according to the manufacturer's directions (Pierce Biotechnology, Inc., Rockford, IL). For quantitation (see Supplemental Figure 2) α-mouse-AP secondary antibody (1:2,500; Promega, Madison, WI) was used in conjunction with ECF substrate (Amersham Biosciences, Piscataway, NJ), and blots were imaged using a Biorad FX phosphoimager (Biorad, Hercules, CA) followed by analysis with QuantityOne software.

Supplemental Figure 1

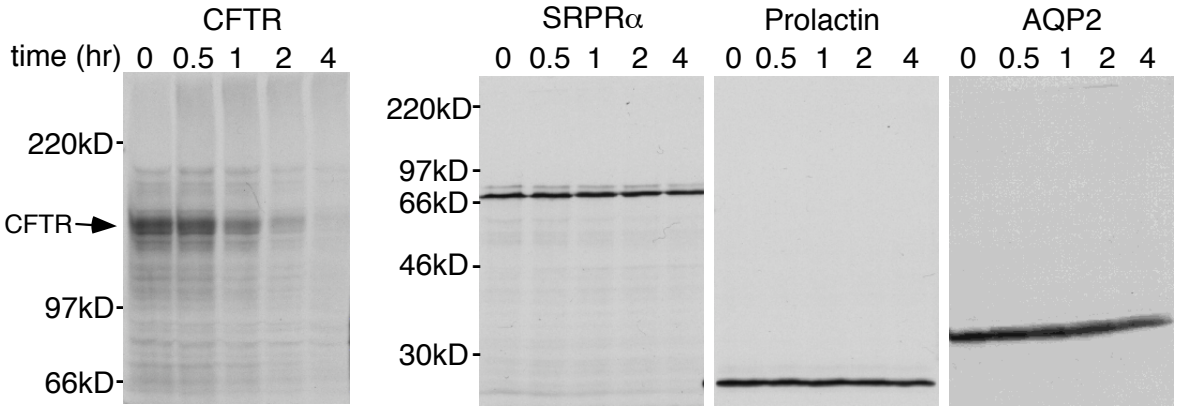

RRL substrate specificity during ERAD. CFTR, SRP receptor α subunit (SRPRα), bovine prolactin and human aquaporin 2 (AQP2) were synthesized in vitro in the presence of microsomal membranes and ^{35}S-methionine. Microsomes were then pelleted, resuspended, and added to degradation reactions as described in Methods. Reactions were incubated at 37˚C for 4h, and aliquots were taken at the indicated time points and analyzed directly by SDS-PAGE and autoradiography. Results show marked differences in the stability between CFTR and the single-spanning, lumenal and six-spanning substrates, respectively. RRL is thus highly specific in discriminating in vitro synthesized proteins as potential ERAD substrates, even those with large cytosolic domains (SRPRα)

Supplemental Figure 2

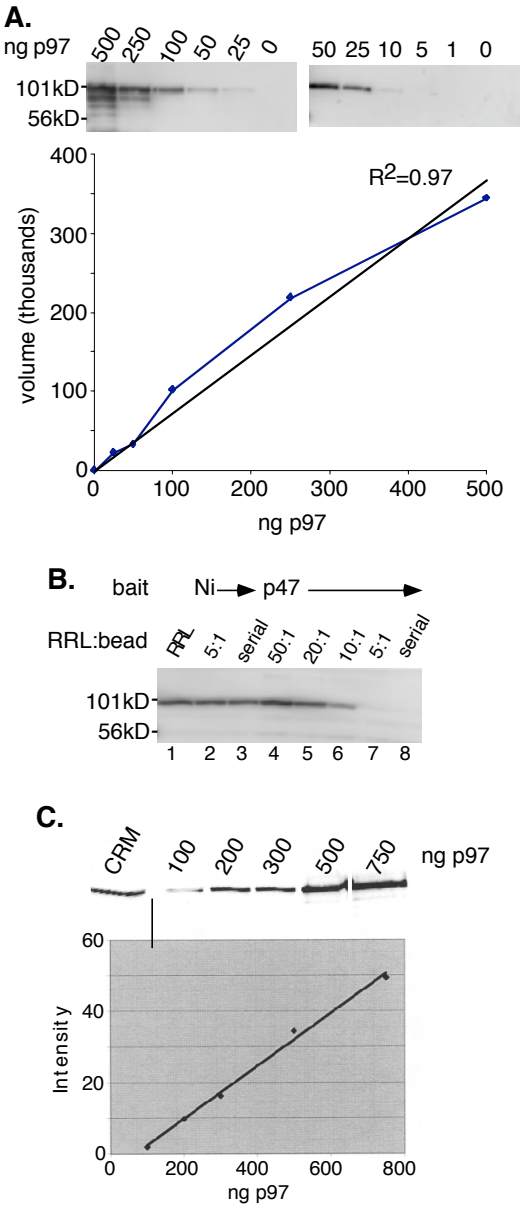

Standard curves for p97 Quantitation. (A) Immunoblots of purified recombinant His6-tagged p97 using mAb anti-p97 (1:500; BD Transduction Laboratories) and 2° anti-mouse-AP (1:2500; Promega) with ECF substrate (Amersham Biosciences). The blot was scanned on a Biorad FX phosphoimager and fluorescent signals were quantitated using QuanityOne software. Plot shows a representative standard curve used to quantitate depletion of RRL p97. Right-hand panel shows decreasing amounts of recombinant p97 with a longer incubation in ECF substrate to determine the limits of detection and compare signals obtained at very low p97 concentrations. **(B)** RRL was incubated for 4 hr at 4° with the indicated ratio (RRL:beads) using Ni-NTA beads (lanes 2-3) or His-tagged p47-saturated Ni-NTA beads (lanes 4-8). In lanes 3 and 8, two serial incubations were performed using 5/1 bead volume each. Depleted RRL was then subjected to immunoblotting as in panels A and B and quantitated against a standard curve of recombinant p97. To ensure that values would fall on the standard curve, RRL in lanes 1-3 were diluted 2 fold. For each RRL depletion, p97 standards were run on the same gel and transferred to the same membrane to ensure similar conditions for immunoblotting. **(C)** A standard curve was developed for microsomal membranes as in A, except that a LICOR Odyssey was used for quantitation. Blots were incubated per manufacturer's instructions, and 2° anti-mouse-Alexa 680 (Molecular Probes) was used. One ml of microsomal membranes was also blotted, and the amount of p97 was quantitated against the standard curve.

Supplemental Figure 3

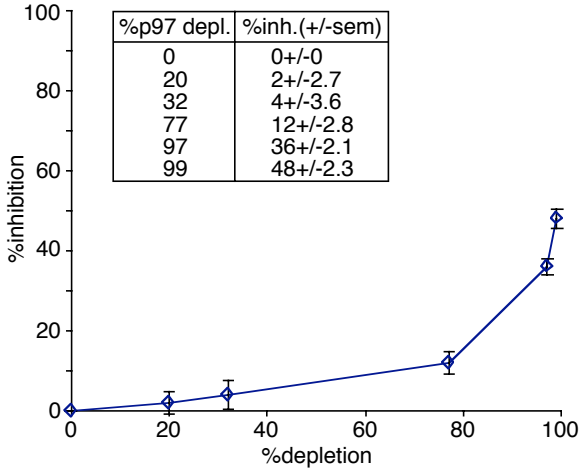

Effect of partial p97 depletion on CFTR degradation activity. RRL p97 was depleted by incubation in varying amounts of p47-saturated Ni-NTA coated beads. Residual p97 was measured by immunoblotting using a standard curve of recombinant protein (inset). CFTR degradation was then measured in depleted RRL based on conversion to TCA soluble fragments as described in Methods. The % inhibition in degradation (based on Mock-depleted RRL) was plotted as a function of the % of p97 depletion. Results show that modest p97 depletion as little effect on CFTR degradation, which likely reflects a relative excess of p97 over substrate and/or ERAD-dependent cofactors. At high levels of depletion (>95%) a linear relationship is observed (see Figure 3E in main text).

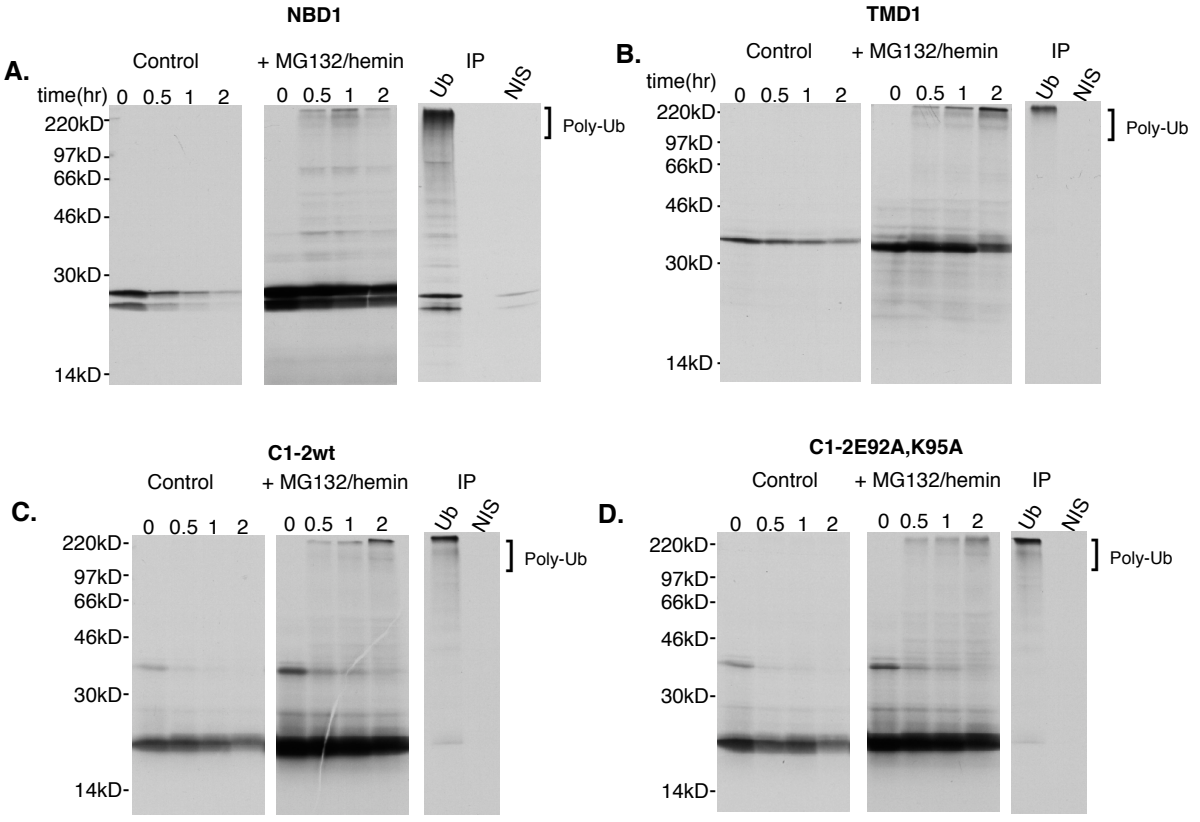

Ubiquitination of CFTR cytosolic and TM domains. Degradation of indicated CFTR domains was carried out under standard conditions (as in Methods) or in the presence of proteasome inhibitors MG132 (100 μM) and hemin (40 μM) as indicated. Aliquots were analyzed by SDS-PAGE and autoradiography at indicated time points. At 2 hours, remaining samples were immunoprecipitated (IP) by incubating overnight at 4°C in 0.1% SDS, 1% NP-40, 10% glycerol, 150mM NaCl, 2mM EDTA, and 25mM Tris-Cl, pH 7.5 in the presence of FK2 anti-polyubiquitin antibody (BioMol) or non-immune serum. Protein G was added for the last hour of incubation, and beads were washed 3 times in IP buffer and analyzed by SDS-PAGE and autoradiography. To better visualize ubiquitinated products, samples containing inhibitors were exposed 4-6 fold longer than controls. Immunoprecipitated products were exposed an additional 10X. For NBD1, MG132 was added directly to translation reactions and incubated at 37°C for 2 hours.

Supplemental Figure 5

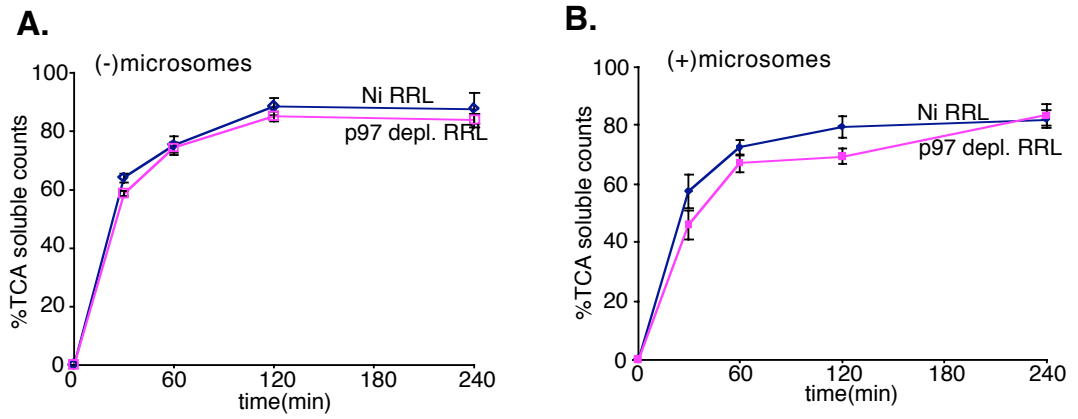

Degradation of NBD1 in presence and absence of microsomal membranes. His-tagged, radiolabeled NBD1 was translated in vitro, isolated and added to degradation reactions containing mock (Ni RRL) or p97-depleted RRL. In panel p97-depleted microsomal membranes were added to recapitulate degradation conditions for TM constructs. Aliquots were taken at the indicated time points, and degradation was determined based on conversion of NBD1 to TCA-soluble fragments. Data show that NBD1 degradation is not significantly affected by the presence or absence of microsomal membranes.